

Integrated System for Sensing and Traverse of Cliff Faces

Terry Huntsberger^{a*}, Vivek A. Sujan^b, Steven Dubowsky^b, and Paul S. Schenker^a

^a Mobility System Concepts Development Section, Jet Propulsion Laboratory,
California Institute of Technology, Pasadena, CA 91109

^b Field and Space Robotics Laboratory, Department of Mechanical Engineering,
Massachusetts Institute of Technology, Cambridge, MA 02139

ABSTRACT

A long duration robotic presence on lunar and planetary surfaces will allow the acquisition of scientifically interesting information from a diverse set of surface and sub-surface sites. The wide range of terrain types including plains, cliffs, sand dunes, and lava tubes will require the development of robotic systems that can adapt to possibly rapidly changing terrain. These systems include single as well as teams of robots. In this paper, we describe the development of an integrated suite of autonomous, adaptive hardware/software control methods called SMART (System for Mobility and Access to Rough Terrain) that enables mobile robots to explore potentially important science sites currently beyond the reach of conventional rover designs. SMART uses the behavior coordination mechanisms of CAMPOUT, a previously developed system for multi-agent control. For the specific application area of cliffside exploration, SMART consists of a distributed sensing system for cooperative map-making called MITSAF (Model-based Information Theoretic Sensing And Fusion), a mobility system for rappelling down a cliff and moving to a designated way-point, and science sample acquisition from the cliff face. We also report the results of some experimental studies on highly sloped cliff faces.

Keywords: Cooperative robots, information theory, unstructured environments, cliff exploration

1. INTRODUCTION

A greater level of rover autonomy is required for a long duration robotic presence on lunar and planetary surfaces. Modular, adaptive robotic systems open up access to a wide range of terrain types including plains, cliffs, sand dunes, and lava tubes (examples shown in Figure 1a and 1c). These systems will include single as well as teams of robots. Recent developments in planetary rover technology^{1,2} have provided capabilities for semi-autonomous robotic traverse over relatively benign terrain. For a conventional wheeled rover, this usually means mobility over continuous natural surfaces having area rock densities of 5-to-10%, modest inclines (<30%), and a hard base with modest soft debris or

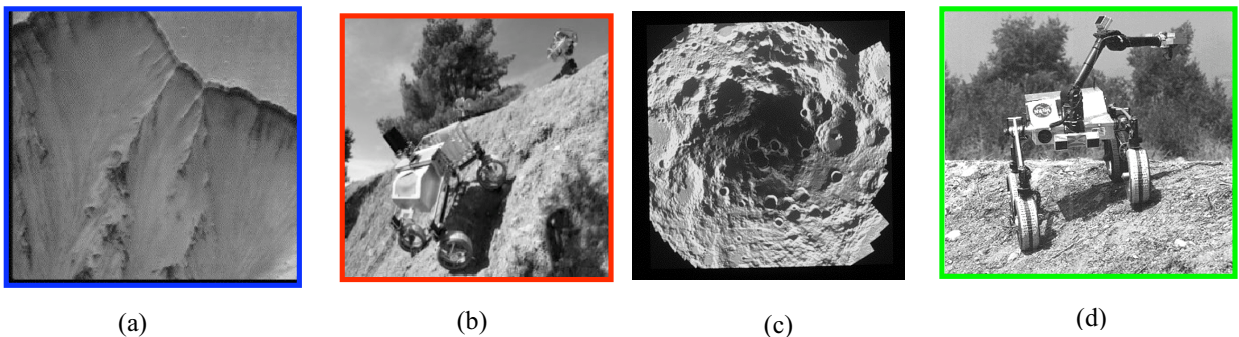


Figure 1. Wide variety of lunar/planetary surface terrains and technology example for autonomous access to high risk, scientifically interesting regions. (a) Mars cliff-face with signs of water outflows; (b) JPL technology prototype cliff-bot ensemble; (c) lunar South Pole-Aitken Basin where signs of water were found by Clementine and Lunar Prospector; (d) JPL technology prototype of an terrain-adaptive reconfigurable rover.

* Further author information: (Send correspondence to Terry Huntsberger, MS82-105, Jet Propulsion Laboratory, 4800 Oak Grove Drive, Pasadena, CA 91109 or e-mail: Terry.Huntsberger@jpl.nasa.gov)

sand pack (i.e., good flotation properties relative to wheel pressures of current rigid chassis designs). Semi-autonomous operation means the rover is sequenced by remote commands usually uplinked once a day, a situation that would not be ideal for outer planet exploration such as that detailed in the recently released Decadal Report.³ This observation even carries through for lunar surface studies using extended long duration rover traverses coupled with in situ analysis and sample return for geological site characterization in order to deconvolve the interplay between tectonic, impact, and volcanic processes.³ Lunar craters less than 14km in diameter tend to have smooth floors, whereas those with larger diameters have a floor that contains widely mixed terrain types. Of particular interest in these lunar and planetary missions is the stratigraphic site history contained in the surfaces that are exposed by the highly sloped terrain.

Our primary objective is the development of an integrated suite of advanced, adaptive hardware/software control methods called SMART (System for Mobility and Access to Rough Terrain) that enables mobile robots to safely move about highly sloped environments and explore potentially important science sites currently beyond the reach of conventional rover designs. The mobility enhancements enabled by SMART are vital for pose reconfiguration for safe access to areas such as those seen in Figure 1c, where the recent Clementine and Lunar Prospector missions indicated the possible presence of water in the Aitken Basin at the south lunar pole, which is extremely rugged terrain and in some places is 13km deep. It is usually possible to build “point,” designs to satisfy the demands from the exploration environment - examples include robots employing legged locomotion,⁴ large inflatable tires, et al. Our approach is to have the robot(s) recognize adverse terrain conditions beyond their nominal operational envelope, and intelligently adapt mobility strategies.^{5,6,7} Two examples are shown in Figure 1b and 1d, where respectively, a cliff-bot is cooperatively driving on a cliff face with the assistance of two anchored tether-bots and a rover reconfigures its shoulder angles and center-of-gravity to enable access to steeply sloped terrain. Enabling such behavior is a dual problem of sensing the conditions that require rover adaptation, and controlling the rover actions as to implement this adaptation in a well understood way (relative to metrics of rover stability, traction, power utilization, etc.).

Our previous related work under the NASA Code R Cross Enterprise Technology Development Program (CETDP) concentrated on developing and testing the components needed for an integrated approach to all terrain exploration (ATE). In FY00, we developed and demonstrated *on-line reconfigurable control* of rover motion and geometry for traverse of challenging terrain (e.g., Mars VL1/VL2-type topographies) and on slopes of up to 50°. ^{6,7} In FY01, we demonstrated a first-of-kind approach to coordinated multi-robot control using *behavior networks* and *publish/subscribe* sharing of distributed state information for way-point navigation on a 70° slope cliff face while maintaining stability (wrt. singularities, tether tension, and rappeller mobility)⁵ implemented under the multi-robot control architecture CAMPOUT (Control Architecture for Multirobot Planetary Outposts).^{8,9,10} The work reported in this paper was done in FY02, where we integrated and demonstrated a *distributed sensing/mobility system* called MITSAF (Model-based Information Theoretic Sensing And Fusion) for mapping, traverse and science data acquisition on a cliff-side wall. MITSAF was developed to address the short-range sensor limitations of a robot traversing a cliff-face for safe navigation. SMART system capabilities for this mission scenario included cooperative map-making and rappelling down a cliff, moving to a designated way-point, and science sample acquisition from the cliff face.

The next section briefly describes the cliff-bot concept and its implementation under CAMPOUT. This is followed by a discussion of the underlying theory and implementation details of the MITSAF intelligent sensing technique used for the map-making and path planning on the cliff-face. Finally, there is a description of our preliminary experiments in the laboratory and field, followed by a summary of results.

2. CLIFF-BOT CONCEPT

Cliff-bot is part of a technology concept developed under SMART for modular robotic exploration of planetary surfaces. The components of the modular robotic system travel as a unit and then autonomously reconfigure themselves as dictated by the terrain. An artist’s depiction of the process is shown in Figure 2. We depart from the systems that use relatively low-level modules in order to build systems with enhanced capabilities^{11,12} in that the components used for our system are full-fledged autonomous vehicles. This approach gives the best mix of mobility for the widest variety of terrain types. The modular cliff-bot system reported in this paper (shown in Figure 3) consists of two anchor-bots that are anchored at the top of the cliff and serve as tether handlers for the vehicle on the cliff-face, a cliff-bot that actively drives on the cliff-face and is stabilized using the dual tethers, and a mobile vehicle at the top of the cliff that can survey the cliff face and provide direction to the cliff-bot. Further details can be found in the paper by Pirjanian, et al.⁵

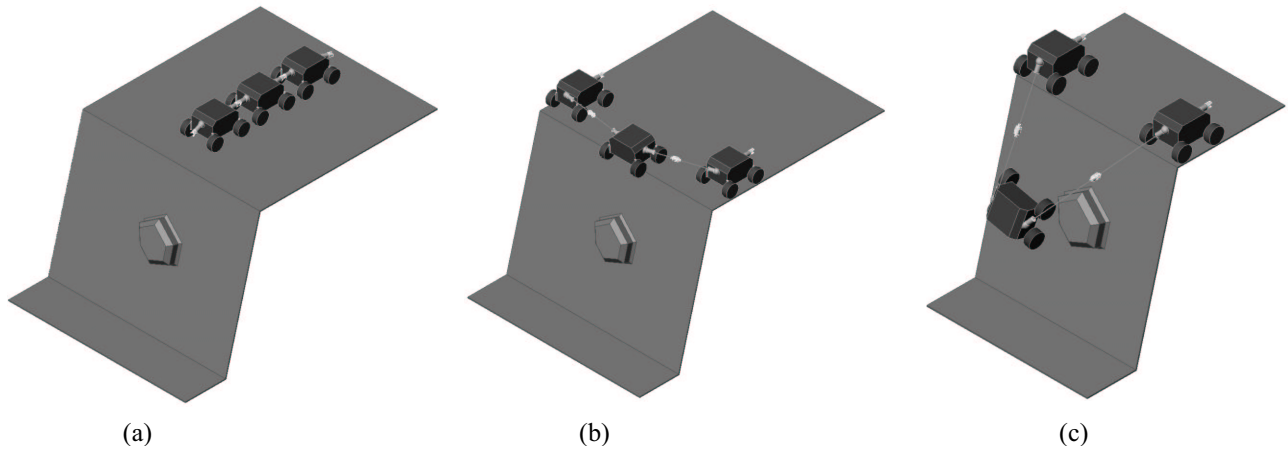


Figure 2. Modular reconfigurable multi-robotic system for traverse of steeply sloped cliff faces. (a) System travels as a unit; (b) reconfigures and positions itself with anchor-bots on either end and a cliff-bot on tethers; (c) cliff-bot traverses the cliff-face.

2.1. Multi-Agent Cliff Access

Figure 3 shows four physically interacting cooperative robots working in an unstructured field environment to assist one robot (cliff-bot) during a traverse on the surface of a cliff face that is not accessible by a single robot alone. Two robots (anchor-bots) act as anchor points for tethers leading down to the cliff-bot, and a fourth robot, RECON-bot (REmote Cliff Observer and Navigator) serves as a mobile observer/sensing module. All robots are equipped with a limited sensor suite, modest computational power and communication bandwidths. The cliff-bot, usually the lightest system, is primarily equipped with a science sensor suite, and short-range sensors for navigation. The RECON-bot autonomously surveys the environment to be traversed by the cliff-bot using maximum information measures to guarantee optimal coverage of the environment, and communicates the relevant data (e.g. for navigation) to the cliff-bot. This system has an independently mobile camera and other onboard sensors to map the environment. Sensing and sensor placement is limited, resulting in uncertainties and occlusions (due to rocks, outcroppings, other robots, etc). Additionally, there is significant task uncertainty in relative pose between the robots and the environment model. Due to these limitations and uncertainties, classical robot control and planning techniques break down.

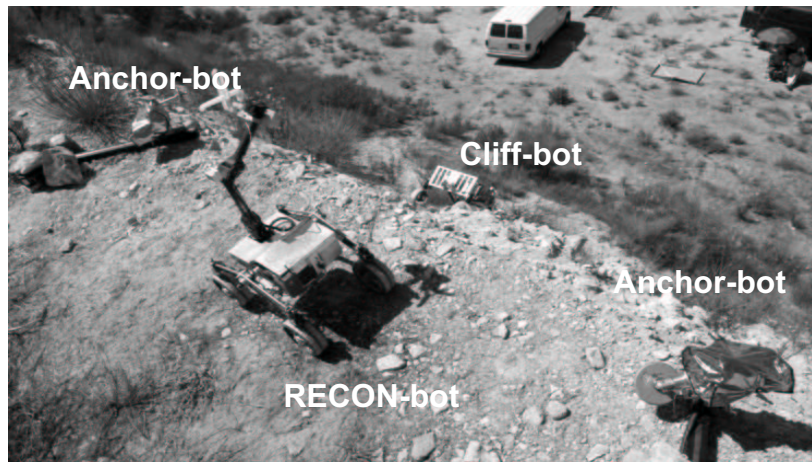


Figure 3. Concept for a cooperative robot cliff descent, consisting of two fixed anchorbots and a tethered cliffbot. RECONbot surveys cliff face from the top edge of the cliff, and passes the path to a chosen goal to the cliffbot.

2.2. CAMPOUT

CAMPOUT^{8,9,10} is currently in use on a suite of JPL robots and has a proven record for real-time, real-world multi-agent control (<http://prl.jpl.nasa.gov>). CAMPOUT is a behavior-based control system that consists of a number of key mechanisms and architectural components that facilitate development of single and multi-robot systems for cooperative and coordinated activities. In general, the CAMPOUT infrastructure defines a network of resources that include plans, behaviors, sensors, and actuators. CAMPOUT uses mechanisms that are based on multiple objective decision theory

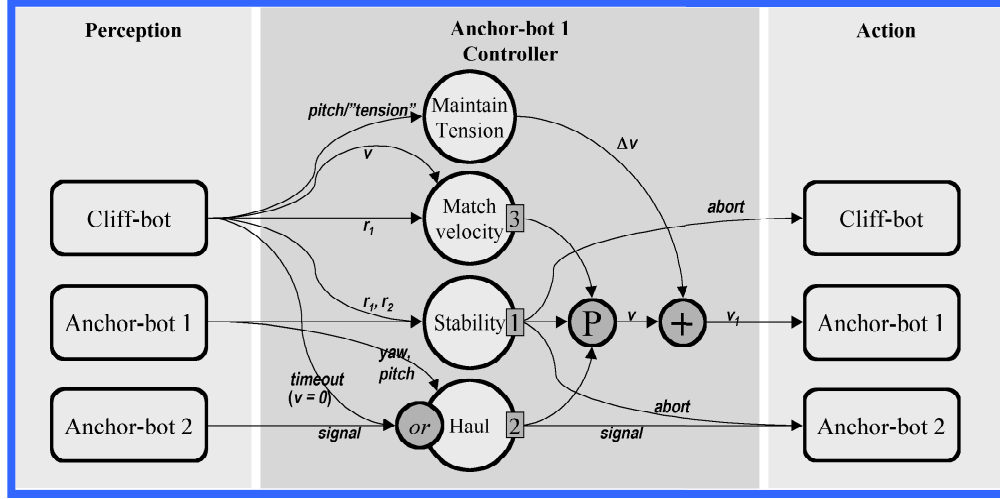


Figure 4. Behavior network for control of tether velocity for Anchor-bot 1. The three behaviors of Match Velocity, Stability, and Haul are fused based on a priority weighting scheme, and then combined with the Maintain Tension behavior using behavior coordination mechanisms in CAMPOUT.

(MODT) to support a sound approach to description and validation of system behavior, thus providing performance guarantees.¹³

Control for a tightly coupled system of three robots negotiating a traverse of a cliff-face requires collective estimation and distributed synchronization. An example of a behavior network for control of one of the anchor-bots is shown in Figure 4, where the mapping from perception to action is accomplished through the behavior coordination mechanisms in CAMPOUT.

There are four main behaviors that govern the tether support for the cliff-bot. These are *Maintain Tension*, used to maintain the tether velocities in order to keep a constant tension; *Match Velocity*, used to regulate the tether velocities based on the current velocity of the cliff-bot on the cliff-face; *Stability*, used to monitor the pitch and roll of the cliff-bot in order to compensate for instability or abort the traversal if the cliff-bot is in potential danger of tip-over; and *Haul*, used to overcome the cliff-bot's inertia at the start of an uphill traverse on a steep slope with an initial tug on the tethers. *Match Velocity*, *Stability*, and *Haul* are all related to cliff-bot safety issues are coordinated through a priority based arbitration scheme (shown as numbered rectangles on the behaviors in Figure 4) under CAMPOUT, with *Stability* having the highest priority followed by *Haul* and *Match Velocity*. All state data is shared between the modules using a publish and subscribe communication protocol.

3. MITSAF

The basic MITSAF algorithm was developed by Sujun.¹⁴ This algorithm fuses sensory information from one or multiple agents using physical sensor/robot/environment models to yield geometrically consistent surrogate information in lieu of missing data. This overcomes the environment, task, robot and sensor uncertainties. Concurrently, the planner/controller efficiently repositions the systems' sensors using an information theoretic approach. Thus sensor positions are planned to help fill in uncertain/unknown regions of the environment model. Sensory information obtained from this process is distributed to the agents. The key idea of the algorithm is to build a common environment model by fusing the data available from the individual robot(s), providing both improved accuracy as well as knowledge of regions not visible by all robots.

3.1. Algorithm Overview

The algorithm consists of three main stages.

Stage 1—In the first stage the system(s) is initialized. This involves initializing the environment map, localizing robots, and generating a first map. In earlier implementations of the MITSAF architecture, the environment map was a 3D probabilistic occupancy grid (each grid voxel value represents the probability that it is occupied).¹⁴ Here, the environment is mapped to a 2.5D elevation grid where each grid cell value represents the elevation at that cell. Next, all

robots contributing to or requiring use of the environment model are localized with respect to the initial environment map. For the cliff exploration task, this includes the cliff-bot and the RECON-bot. Localization can be achieved by either (a) external localization—mapping a common target visible by all robots; or (b) internal localization—mapping fiducials on all robots by other robot team members where one robot is selected as the origin. We use internal localization for this task, with the RECON-bot localizing the cliff-bot with respect to its start position—the origin. Subsequently, a first environment scan is done by the RECON-bot. Each environment point mapped is fit as an elevation at the corresponding grid cell.

Stage 2—In the second stage, the cliff edge is identified by the RECON-bot. This edge is parameterized by a best-fit non-convex polygon, with a tolerance based on the RECON-bot wheel diameter. This permits the RECON-bot to traverse a geometrically complex cliff edge without falling over. In cliff edge parameterization, the surface currently in contact with the RECON-bot is identified in the environment model. This surface is then approximated by a best-fit polygon. The tolerance of the fit is limited by the known rover wheel diameter (fit tolerance = wheel characteristic length/length per grid cell). For this the incomplete environment model is temporarily completed by a Markovian approximation for unknown grid cells. In the Markovian approximation, a worst case initial guess is assumed for all unknown points. This value is the lowest elevation value currently in the known model. A nearest measured neighbor average is performed and iterated till convergence.

Using the Markovian approximation of the environment, the current rover contact surface (called the plateau) is first identified. This is achieved by setting a height threshold bound to the environment model and projecting the resulting data set onto the XY plane, followed by a region growing operation around the current known rover coordinates. Next, the binary image is smoothed by a mathematical morphology close operation (dilation + erosion). Plateau edge pixels are identified at this stage. However, to remove small holes in the plateau, an edge following operation is performed, yielding a single closed loop of boundary pixels. Finally, this set of points is parameterized by a closed polygon. This is initiated by fitting the full set of boundary pixels to a straight line. For any given subset of boundary pixels that is currently fit to a line, if the error bound on this fit exceeds the prescribed tolerance, then the pixel set is divided into two, and the process is repeated. However, before error bound evaluation, line segments fit to each subset of boundary pixels, are joined to form a closed polygon.

Stage 3—In the third stage, the MITSAF planner, controller and sensor fusion modules select new vision sensor positions for the model “building,, agents (i.e. RECON-bot), reposition the system for optimal viewing, and resolve the true new position for accurate data fusion. A rating function is used to determine the next pose of the camera from which to look at the unknown environment. The aim is to acquire new information about the environment that would lead to a more complete environment map. In selecting this new camera pose the following four constraints are considered:

- (i) *Goal configuration is unoccupied*
- (ii) *Goal reached by a collision free path*
- (iii) *Goal configuration should not be far from the current one*—a Euclidean metric in configuration space is used to define the distance moved by the camera.
- (iv) *Measurement at the goal configuration should maximize information intake*—the new information H is equal to the expected information of the unknown/partially known region viewed from the camera pose under consideration. This is based on the known obstacles from the current environment model, the field of view of the camera and a framework for quantifying information. Shannon’s information content measure is extended to a 2.5D signal-environment elevation map. The new information content for a given camera view pose is given by:

$$H(\text{cam}_{x,y,z,c_p,c_y}) = \sum_I \left(\frac{n_{grid}^i}{n_{grid}^{max}} \right) \left(\frac{P_V^i}{2} \log_2 \frac{P_V^i}{2} + \left(1 - \frac{P_V^i}{2} \right) \log_2 \left(1 - \frac{P_V^i}{2} \right) \right) \quad (1)$$

where H is summed over all grid cells i visible from camera pose $\text{cam}_{x,y,z,c_p,c_y}$, n_{grid}^i is the number of environment points measured and mapped to cell I , n_{grid}^{max} is the maximum allowable mappings to cell I , and P_V^i is the probability of visibility of cell i from the camera test pose given. P_V^i is evaluated by computing the likelihood of occlusion of a ray $\text{ray}_{x,y,z}$ using the elevation, $\text{Ob}_{x,y,z}$, and the associated uncertainty, $\text{U}_{x,y,z}$, at all cells lying along this ray path shot through each position in the environment grid to the camera center. This is given by:

$$P_V^i = \left(\frac{\text{sgn}(\text{ray}_z - \text{Ob}_z)}{2} + \frac{1}{2} \right) \exp\left(-\frac{z^2}{2\sigma_z^2}\right) dz \quad (2)$$

This definition for H behaves in an intuitively correct way, in that regions with higher visibility and higher levels of associated unknowns yield a higher expected H value, and more highly occluded or better known regions result in lower expected H values.

During the mapping process some regions expected to be visible may not be. This may be attributed to sensor characteristics (e.g. lack of stereo correspondence due to poor textures or lighting conditions) and inaccuracies in the data model (e.g. expected neighboring cell elevations and uncertainties—occlusions). However, after repeated unsuccessful measurements of cells expected to be visible, it becomes more likely that sensor characteristics are the limitation. This limitation is addressed in MITSAF using a data quality function that decreases as the number of unsuccessful measurements of the visible cell increases. The probability of visibility of the cell i , P_V^i , is pre-multiplied by an “interest,” function for the cell i in order to minimize the number of times that a region is visited without successfully obtaining more information.

A final step in environment map building is to identify the motion of the camera. This process eliminates manipulator positioning errors and vehicle suspension motions, and allows for accurate data fusion. Spatial points in the reference frame are selected and tracked based on a Forstner interest operator and a homography transform² which results in a set of linear equations that can be solved using conventional techniques. The least mean square error solution to this set of equations is used in combination with a recursive method to determine the mean and covariance of the rotational and translational components of the transform. This essentially maintains a measure on how certain the camera motion is w.r.t. its original configuration (assuming the original configuration is known very precisely w.r.t. the common reference frame).

This three phase algorithm will produce a 2.5D map that is optimized for maximal information content within the mission time and power resource constraints, and which can be used by the RECON-bot to plan a safe path to potential science targets on the cliff-face. In order to maximize the use of limited communication bandwidth between the RECON-bot and cliff-bot, a safe path consisting of a number of positional waypoints is the only information passed to the cliff-bot. The cliff-bot uses its short-range sensors for additional obstacle avoidance during the traverse of the cliff-face. The next sub-section gives brief details of the ROAMAN (ROAd MAp Navigation) algorithm² that is used for this process.

3.2. Safe Path Planning to Goal

The range of the stereo hazard cameras on the cliff-bot is typically 1 to 1.5 meters, which could lead to a entrapment problem for long traverses on cliff-faces. Long range path planning on the cliff-face is done by the RECON-bot using the optimized map that has been generated by Phases 1-3 of MITSAF. The RECON-bot autonomously generates a series of waypoints using ROAMAN that are passed to the local path planning algorithm (DriveMaps) for local obstacle avoidance during the traverse of the individual legs. Both the long and short range portions of the algorithm use an occupancy grid representation to perform hazard detection and path planning. The algorithm is not guaranteed to generate an optimal shortest path, but will maintain the safety of the rover. A traversability map generation process similar to that in Singh, et al.¹⁵ is used to generate a labeled map of potential hazards. A 1D medial axis or Voronoi transform for each row of the grid similar to that in Wilmarth, et al.¹⁶ and Choset¹⁷ is performed to mark the center spots between hazards. The rover footprint is virtually driven on the paths as they develop in order to maintain safety in the event that a turn might be necessary. A depth first search algorithm is run to find the longest connected paths, followed by a least squares fit to the longest connected path in order to determine waypoints for the traverse. After receipt of the navigation waypoints, the cliff-bot then autonomously performs the traverse using its hazard cameras for local path planning and obstacle avoidance. Further details about ROAMAN can be found in Huntsberger, et al.²

4. EXPERIMENTAL STUDIES

We conducted a number of experimental studies in the Planetary Robotics Laboratory (PRL) at JPL, and in the field at a cliff-site near the Tujunga Dam in Tujunga, CA. The experimental setup for the first study in the PRL is shown in Figure 5, where the Sample Return Rover (SRR), a JPL technology prototype, is acting in the role of the RECON-bot discussed in the text. The SRR is a four-wheeled mobile robot with independently steered wheels and independently controlled shoulder joints. A stereo pair of cameras (15cm baseline, individual camera 45° field-of-view) is mounted on a four degree-of-freedom manipulator at the front of the SRR. The SRR is equipped with a 266 MHz Pentium II

processor in a PC-104+ stack configuration and operates under the real-time OS VxWorks5.4. Five mapping techniques were implemented with increasing levels of sophistication. These include:

1. Raster scanning without mast-based camera panning
2. Raster scanning with mast-based camera panning
3. Information based environment mapping with cliff edge assumed to be a straight line segment
4. Information based environment mapping with cliff edge approximated as a non-convex polygon
5. Information based environment mapping with interest function and cliff edge approximated as a non-convex polygon

Methods 1 and 2 reflect commonly used mapping schemes used on NASA missions. Methods 3, 4 and 5 reflect with increasing complexity the algorithms discussed in this paper.

Figure 6 shows the number of environment grid cells explored as a function of the number of stereo imaging steps. From this, the improved efficiency of the method presented in this paper over conventional raster scanning methods can be seen, with an order of magnitude more points being mapped by Method 5 over those returned from Method 1 for the same number of stereo imaging steps. Additionally, a significant improvement in efficiency is noted while progressing from Method 3 to Method 5. In Method 4, by parameterizing the cliff edge, the rover is able to follow the edge more aggressively, thus covering a larger variety of view points. Further, it is observed that the left region of the sandpit in Figure 5 yields poor data (due to lack of stereo correspondence). Since this region is expected have high information content (due to lack of occlusions), the algorithm in Method 3 tends to converge to view points looking in that direction. However, in Method 5, the algorithm concludes that the data quality is poor and eventually loses interest in this region. Figure 7 shows an overhead view of the mapped area with Method 3 on the left and Method 5 on the right. Method 5 maps approximately twice the spatial region and has denser coverage as

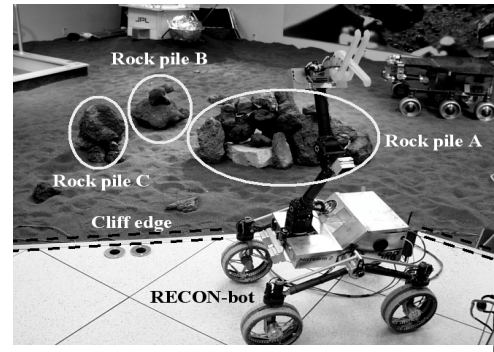


Figure 5. Experimental setup in PRL at JPL with SRR as a RECON-bot, three rock piles, and a small step edge (marked with dotted lines) serving as the cliff-edge.

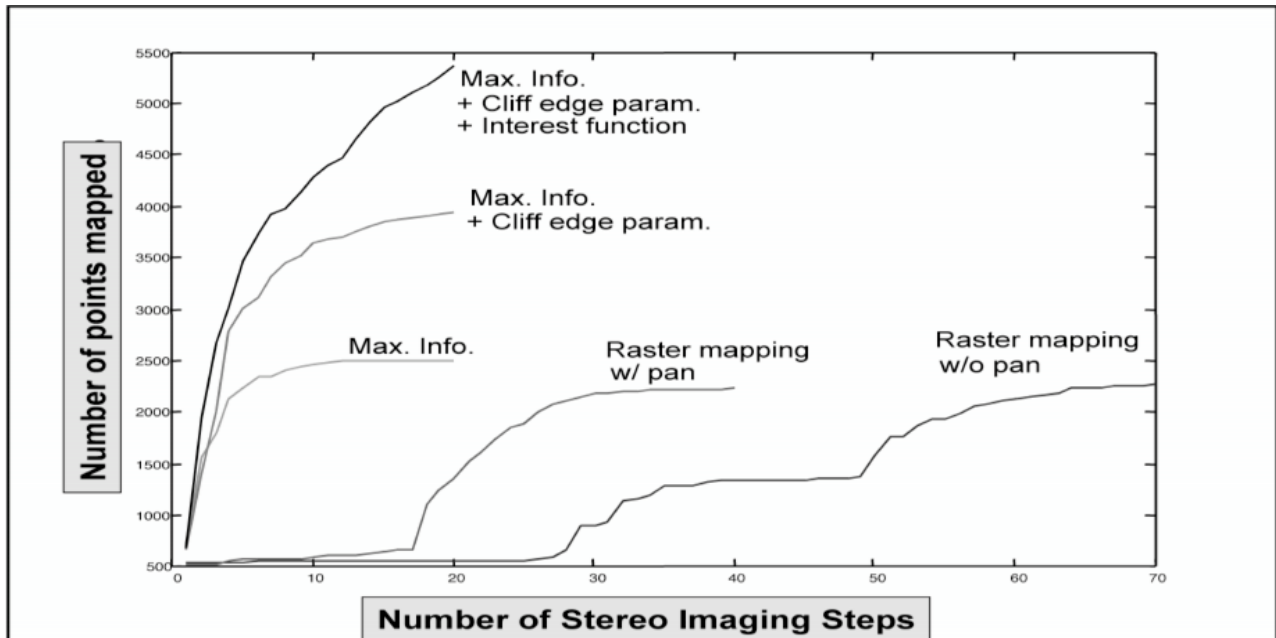


Figure 6. Comparison of the five control methods for efficiency of environment coverage versus the number of imaging steps. An order of magnitude increase in the number of points mapped for the same number of imaging steps is seen when going from the simple Method 1 of raster mapping without any camera pan to Method 5 with camera pose control by maximum information content, cliff edge parameterization, and interest function.

compared to Method 3 in the same number of imaging steps.

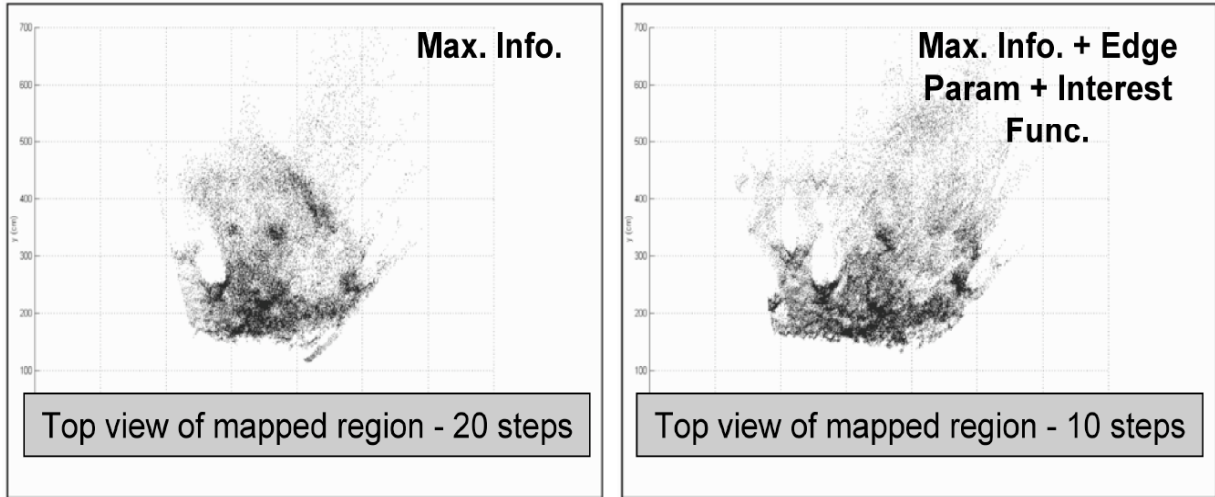


Figure 7. Comparison of relative efficiency of mapping between (left) Method 3 using maximum information content alone; (right) Method 5 using maximum information content, cliff-edge parameterization, and an interest function. Spatial coverage is twice as dense in half the number of imaging steps.

The Tujunga Dam cliff-site used in the second experimental study is shown in Figure 8, where the goal point and potential obstacles are labeled in Figure 8a shot from the bottom of the cliff, and Figure 8b is shot from the top of the cliff. The average terrain slope in the study area on the cliff was 79° . Once again, the SRR is playing the role of the RECON-bot at the top of the cliff. A representative stereo pair taken with the navigation cameras on the SRR end effector is shown in Figure 9. The cliff edge (shown with arrow in Figure 9) was marked by the algorithm as any area in the image with a slope greater than 45° . Due to time constraints, we were only able to run the experimental tests for Method 4 using the maximum information content and Method 5 using the maximum information content with interest

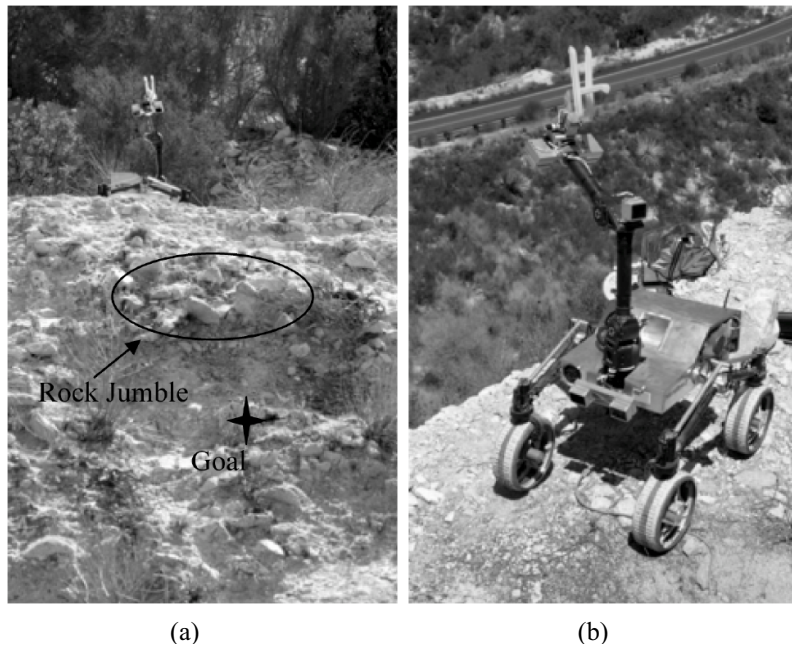


Figure 8. Tujunga Dam cliff-site used in second experimental study. (a) View from bottom of cliff, with obstacles marked with oval and goal marked with a star; (b) view from the top of the cliff.

function. The results of the study for 10 imaging steps is shown in Figure 10. Comparison with Figure 6 where the gain in environment coverage between the two techniques is 100% and Figure 10 where the gain is only 30% indicates that the stereo maps are better in the laboratory environment due to more controlled lighting and contrast conditions. We ran the ROAMAN path planning algorithm on the 2.5D labeled grid map using a goal position selected from the surveillance imagery (marked with a star in Figure 8), and produced a safe path to the goal as shown in Figure 11. Although the labeled cells are sparse, the ROAMAN algorithm found a single path to the goal. Unfortunately, time constraints precluded us from exercising this path to the goal on the cliff-face.



Figure 9. Representative left and right images at the Tujunga Dam site from the stereo navigation cameras on the end effector of the RECON-bot positioned at the top edge of the cliff. Stereo disparity is used to determine the cliff-edge (shown with arrow) for image acquisition planning purposes.

5. SUMMARY AND CONCLUSIONS

We have presented an integrated approach to navigation called SMART that is used for the control of modular reconfigurable robotic systems. Its utility for analysis of and access to rough, highly sloped terrain was demonstrated using a cliff-bot scenario. A surveillance rover was incorporated into the mobility portion of the system using an algorithm called MITSAF, that optimizes the use of system resources for mapping through rover mobility and pose control based on information content measures. The algorithm demonstrated an order of magnitude increase over raster based scanning methods in the coverage of the environment. The ROAMAN long range path planning algorithm was used to plan a safe path with waypoints around an obstacle to a pre-selected goal on the Tujunga Dam cliff-face. Due to time constraints, we were only able to demonstrate a precision approach to a science target on the cliff-face mockup in the PRL at JPL. We plan to return to the field and complete the traverse to the goal and to collect data for a comparison between the five methods detailed in the text. In addition, we are examining limbed designs¹⁸ for advanced systems that will enable access to cliff-face areas such as overhangs and vents that are even beyond those demonstrated in the present paper.

ACKNOWLEDGMENTS

The research described in this paper was carried out at the Jet Propulsion Laboratory, California Institute of Technology, under a contract with the National Aeronautics and Space Administration. The assistance of members of the Planetary Robotics Laboratory in conducting experimental trials with the cliff-bot system is greatly appreciated. The portion of this work done by MIT is supported by the NASA Jet Propulsion Laboratory under contract number 1216342.

REFERENCES

1. P.S. Schenker, T.L. Huntsberger, P. Pirjanian, E.T. Baumgartner, and E. Tunstel, "Planetary rover developments supporting Mars science, sample return and future human-robotic colonization," *Autonomous Robots*, **14**, pp. 103-126, 2003.
2. T. Huntsberger, H. Aghazarian, Y. Cheng, E. T. Baumgartner, E. Tunstel, C. Leger, A. Trebi-Ollennu and P. Schenker, "Rover Autonomy for Long Range Navigation and Science Data Acquisition on Planetary Surfaces," in *Proc. 2002 IEEE International Conf. on Robotics and Automation (ICRA2002)*, pp. 3161-3168, 2002.

3. *The Future of Solar System Exploration, 2003-2013*, Ed. Mark V. Sykes, NRC Planetary Decadal Report, 2002 (<http://www.aas.org/~dps/decadal>).
4. D. Apostolopoulos and J. Bares, "Locomotion configuration of a robust rappelling robot," in *Proc. IEEE/RSJ (IROS'95)*, pp. 280-284, 1995.
5. P. Pirjanian, C. Leger, E. Mumm, B. Kennedy, M. Garrett, H. Aghazarian, P. S. Schenker, and S. Farritor, "Distributed Control for a Modular, Reconfigurable Cliff Robot," in *Proc. 2002 IEEE International Conf. on Robotics and Automation (ICRA2002)*, pp. 3136-3141, 2002.
6. P. S. Schenker, P. Pirjanian, B. Balaram, K. S. Ali, A. Trebi-Ollennu, T. L. Huntsberger, H. Aghazarian, B. A. Kennedy, E. T. Baumgartner, K. Iagnemma, A. Rzepniewski, S. Dubowsky, P. C. Leger, D. Apostolopoulos, and G. T. McKee, "Reconfigurable robots for all terrain exploration," in *Proc. SPIE Sensor Fusion and Decentralized Control in Robotic Systems III*, **4196**, 2000.
7. K. Iagnemma, A. Rzepniewski, S. Dubowsky, P. Pirjanian, T. Huntsberger, and P. Schenker, "Mobile robot kinematic reconfigurability for rough-terrain," in *Proc. SPIE Sensor Fusion and Decentralized Control in Robotic Systems III*, **4196**, 2000.
8. T. Huntsberger, P. Pirjanian, A. Trebi-Ollennu, H.D. Nayar, H. Aghazarian, A. Ganino, M. Garrett, S.S. Joshi, and P.S. Schenker, "CAMPOUT: A Control Architecture for Tightly Coupled Coordination of Multi-Robot Systems for Planetary Surface Exploration," to appear in *IEEE Transaction on Systems, Man, & Cybernetics: Special Issue on Collective Intelligence*, 2003.
9. P. Pirjanian, T. Huntsberger, A. Trebi-Ollennu, H. Aghazarian, H. Das, S. S. Joshi, and P. S. Schenker, "CAMPOUT: A control architecture for multirobot planetary outposts," in *Proc. SPIE Conf. Sensor Fusion and Decentralized Control in Robotic Systems III*, **4196**, pp. 221-230, 2000.
10. P. Pirjanian, T.L. Huntsberger, and P. S. Schenker, "Development of CAMPOUT and its further applications to planetary rover operations: A multirobot control architecture," in *Proc. SPIE on Sensor Fusion and Decentralized Control in Robotic Systems IV*, **4571**, pp. 108-119, 2001.
11. M. Yim, "PolyBot: A modular reconfigurable robot," in *Proc. IEEE Int. Conf. on Robotics and Automation (ICRA'00)*, pp. 514-520, 2000.
12. D. Rus, "Self-reconfiguring robots," *IEEE Intelligent Systems*, **134**, pp. 2-4, 1998.
13. P. Pirjanian, "Multiple objective behavior-based control,,," *Journal of Robotics and Autonomous Systems*, **31**(1-2): pp. 53-60, 2000.
14. V. A. Sujan, *Compensating for Model Uncertainty in the Control of Cooperative Field Robots*, Ph.D. Thesis, Dept. of Mech. Eng., MIT, Cambridge, MA., June 2002.
15. S. Singh, R. Simmons, M.F. Smith, III, A. Stentz, V. Verma, A. Yahja, and K. Schwehr, "Recent progress in local and global traversability for planetary rovers," in *Proc. IEEE Int. Conf. on Robotics and Automation (ICRA'00)*, pp. 1194-1200, 2000.
16. S. A. Wilmarth, N. M. Amato, and P. F. Stiller, "MAPRM: A probabilistic roadmap planner with sampling on the medial axis of the free space," in *Proc. IEEE Int. Conf. on Robotics and Automation (ICRA'99)*, Detroit, MI, pp. 1024-1031, 1999.
17. H. Choset, *Sensor Based Motion Planning: The Hierarchical Generalized Voronoi Graph*, Ph.D. thesis, California Inst. of Tech., 1996.
18. B. Kennedy, H. Agazarian, Y. Cheng, M. Garrett, G. Hickey, T. Huntsberger, L. Magnone, C. Mahoney, A. Meyer, J. Knight, "LEMUR: Legged Excursion Mechanical Utility Rover," *Autonomous Robots*, **11**(11), pp. 201-205, 2001.

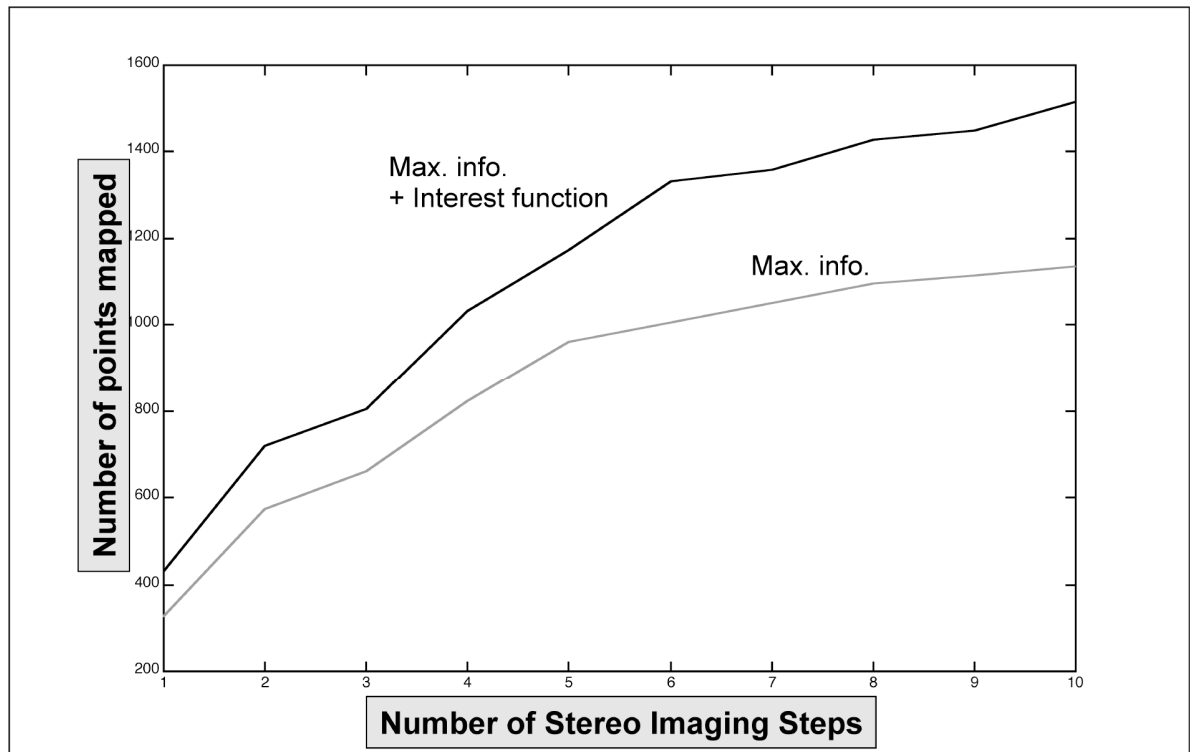


Figure 10. Comparison of the mapping of the cliff-face for Method 3 using maximum information content, and Method 4 using maximum information content and an interest function. The increase in the number of points mapped is about 30% for the same number of imaging steps.

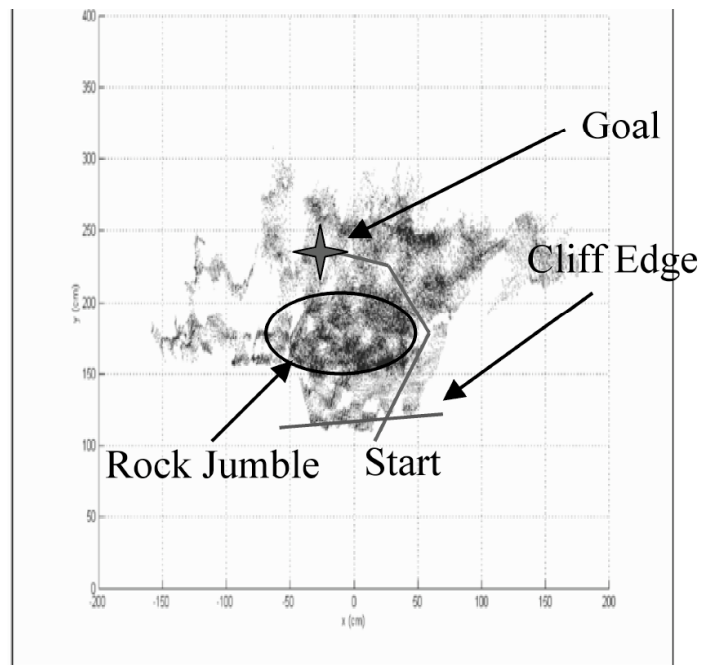


Figure 11. ROAMAN path plan overlaid on overhead view of Tujunga Dam cliff-face looking from the top edge, with goal position and obstacles as shown in Figure 9. ROAMAN used portion of map with densest 2.5D labels, thus favoring the path to the right of the obstacles over the left due to the lack of valid range data in that area.